RESEARCH PAPER

Dimethylamine Controlled Sol-Gel Process to Grow ZnO Nanorods

Dhanashri Gajanan Patil, Vinita Vikas Deo, Shanabhau Damu Bagul, Priyanka Ashok Patil, Prabhakar Sandu Sonawane, Madhav Sitaram Wagh*

Nanomaterials Research Lab, Department of Physics, Pratap College, Amalner, Maharashtra, India.

ARTICLE INFO

Article History:
Received 10 November 2017
Accepted 16 December 2017
Published 01 January 2018

Keywords:
Nanostructures
Nucleation
Sol-gel growth
ZnO nanorods

ABSTRACT

ZnO nanorods were prepared using dimethylamine (DMA) controlled Sol-Gel process. Dimethylamine was added as an additive to control the sol-gel process for growing ZnO nanorods. DMA would exhibit stabilizing effect, promote dissolution of precursor and control the rate of sol-gel reactions because of its basic nature and significant miscibility. The Structural and microstructural properties of the powders were characterized by X-Ray Diffractometer (XRD), Field Emission Scanning Electron Microscopy (FESEM) and Transmission Electron Microscopy (TEM). FESEM and TEM analysis revealed that the ZnO powder prepared were nanorods in nature. The optical properties of powders were characterized by UV-Visible and Photoluminescence (PL) spectroscopy. The Structural, morphological, optical and photoluminescence properties of so obtained ZnO powders consisting of nanorods were studied. DMA is simple amine but found to be very effective to control the aspect ratio of nanorods. The role of DMA in growing wurtzite structured hexagonal ZnO nanorods with [0001] orientation was interpreted and growth mechanism of ZnO nanorods was explained.

How to cite this article
Patil D. G, Deo V. V, Bagul S. D, Patil P. A, Sonawane P. S, Wagh M. S. Dimethylamine Controlled Sol-Gel Process to Grow ZnO Nanorods. J Nanostruct, 2018; 8(1):11-20. DOI: 10.22052/JNS.2018.01.002

INTRODUCTION

Zinc oxide (ZnO) has become one of the most important functional material with unique properties, such as, wide direct band gap (Eg = 3.37 eV, n type), high transparency in visible and IR region, intrinsic dipole moment in its Wurtzite structure - responsible for polarity in basal (Zn/O) terminated planes and formation of preferred orientation [1], electric conductivity, piezoelectricity etc. More interestingly, ZnO nanostructures exhibit fascinating morphologies, such as, nanorods [2], nanotubes [3] and nanowires [4] etc. Due to these properties, ZnO has found vast commercial applications, such as, solar cells [5-6], photo detectors [7], light emitting diodes [8] , ultraviolet Lasers [9], optical modulator wave guide [10], chemical gas sensors [11] etc. Various fabrication techniques have, therefore, been employed to grow ZnO nanowires [12- 32].

Among the chemical methods, sol-gel process is of great interest due to its simplicity, reproducibility, cost effectiveness and having no need of critical conditions in terms of pressure, vacuum or temperature. One of the components of the ZnO sol-gel process is the additive, commonly known as stabilizer that has different roles such as reacting with precursor, facilitating the formation of nanorods. Aliphatic amines could be widely used as additives in sol-gel process because of their basic nature, significant miscibility with organic

* *Corresponding Author Email: wmadhav19@gmail.com*

solvents like alcohols, exhibiting stabilizing effect, promoting dissolution of precursor, controlling the rate of sol-gel reactions, lowering the chance of impurities to contaminate ZnO structure. Dimethylamine (DMA) has been used first time in the present investigation as an additive in sol-gel process to synthesize nanorods. To the best of our knowledge, any researches concerning the effect of DMA as an additive on sol-gel behavior and properties of DMA controlled sol-gel derived ZnO nanorods has never done before. In present investigation, the effect of variation of amount of DMA added into zinc acetate solution on the behavior of sol-gel process and hence on the growth morphology of ZnO nanostructures have been studied. Using characterization techniques, the influence of DMA on structural, microstructural, optical and photoluminescence properties is studied.

MATERIALS AND METHODS

Experimental procedure

ZnO nanorods were prepared through sol-gel process. AR grade Zinc acetate (ZA-($Zn(CH_3COO)_2 \cdot 2H_2O$)) was used as zinc source and dimethylamine (DMA- $(CH_3)_2NH$)) was used as an additive to control the sol-gel process. 40 ml zinc acetate (2.25M) and 50 ml DMA (2.25M) solutions were prepared in double distilled water. Different samples were prepared by adding slowly different amounts of DMA into 40 ml zinc acetate solution with continuous stirring and heating at 60^0C. The final solutions gave either precipitate or sol depending on the amount of DMA added into the starting solution of zinc acetate. The experiments were conducted by varying the ratio of DMA solution to zinc acetate solution as: 1:40, 1:20, 1:13, 1:10, 1:8, 1:7, 1:5, 1:2. Of these eight, first four ratios (1:40, 1:20, 1:13, 1:10) did not give either the precipitation or the sol. From latter four ratios (DMA to zinc acetate), the 1:8 ratio gave immediate precipitation and the ratios: 1:7, 1:5, 1:2 gave soft gel, proper gel and dense gel respectively. The so obtained precipitate and each sol (gel after aging) were dried at 200 ^{0}C for 4 h and then fired at 500 ^{0}C for 1 h. The powders obtained from the ratios: 1:8, 1:7, 1:5, 1:2 were referred to as: S1, S2, S3 and S4 respectively. Proper gel was formed when the ratio was 1:5 (8 ml DMA solution added into 40 ml zinc acetate solution). This was the optimum condition for formation of proper gel. The experimental conditions are summarized in Table 1.

Experimental Characterization techniques employed to study the samples

The samples: S1, S2, S3 and S4 were studied using various characterization techniques. X-ray diffraction (XRD) technique (D8ADVANCE Bruker AXS) was employed to characterize the orientation and crystallinity of ZnO nanostructures using Cu Kα radiation with a wavelength 1.5418 Å. Field emission scanning electron microscope (FE-SEM: Hitachi S-4800- coupled with energy dispersive (EDAX)) spectrometer was used to analyze the morphology and chemical composition of the ZnO nanostructures. Transmission electron microscopy (TEM) was used to obtain exact particle size of the material. Optical studies, using UV-Vis spectrophotometer (Shimadzu UV-2450), were performed in the wavelength region 300- 600 nm to determine the band gap energy of the sample powders. Photoluminescence spectra of the samples were recorded on Fluorescence spectrometer (LS 55, Perkin-Elmer) with excitation wavelength of 310 nm.

RESULTS AND DISCUSSION

Structural properties using X Ray Diffraction technique

X-ray diffraction spectra of S1, S2, S3 and S4 samples are represented through Figs. 1(a), 1(b), 1(c) and 1(d) respectively. Observed XRD peaks of all samples match with peaks reported in standard JCPDS data (JCPDS 36-1451). The XRD spectra confirmed the sample powders to

Table 1. The experimental conditions to get ZnO nanostructures of different morphologies.

Sample	DMA (ml)	ZA (ml)	DMA: ZA Ratio	Gel Status	Gel Setting time
S1	5	40	1:8	Immediate ppt	5 min
S2	6	40	1:7	Soft gel	60 min
S3	8	40	1:5	Proper gel	30 min
S4	20	40	1:2	Soft gel	21 days

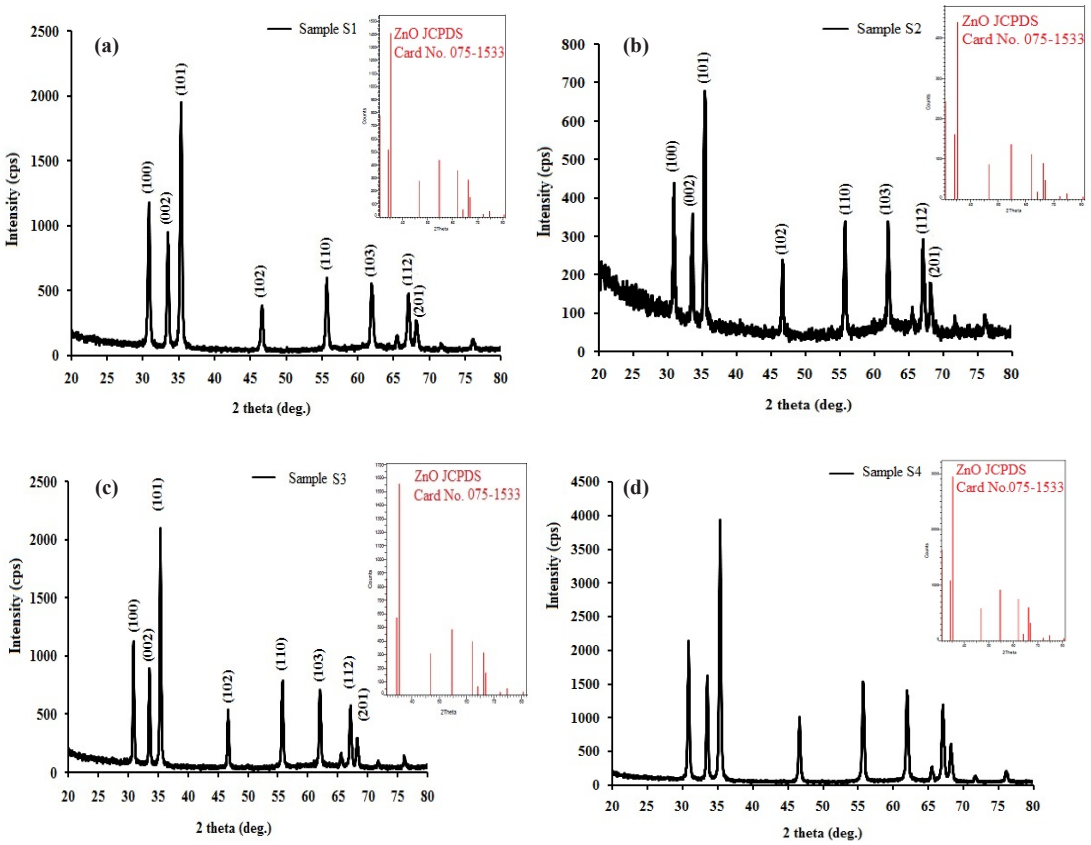

Fig. 1. (a) XRD Spectrum of S1 (b) XRD Spectrum of S2 (c) XRD Spectrum of S3 (d) XRD Spectrum of S4

be the wurtzite phase of ZnO. The observed relative intensities of the peaks are larger than the intensities of corresponding peaks of the standard JCPDS card measured from randomly oriented powder samples. It may be due to preferred orientation of the sample planes. The degree of preferred orientation in case of (002) plane can be determined by the relative texture coefficient (TC) [33], which is given by equation (1):

$$TC_{002} = \frac{I_{002}/I^{o}_{002}}{I_{002}/I^{o}_{002}+I_{101}/I^{o}_{101}} \quad (1)$$

where TC_{002} is the texture coefficient of diffraction peak (002) over (101), I_{002} and I_{101} are measured intensities of peaks due to (002) and (101) planes respectively and I^{o}_{002} and I^{o}_{101} are corresponding intensities of peaks reported by standard JCPDS card for randomly oriented ZnO powder. The TC of randomly oriented material is 0.5, while the TC values calculated for S1, S2, S3 and S4 samples are: 0.56, 0.56, 0.52 and 0.52 respectively. These values indicate that the structure of ZnO nanostructures may have a preferential orientation along the c axis. Average particle sizes of samples S1, S2, S3 and S4 calculated by using Debye-Scherrer Formula are: 10.70 nm, 11.59 nm, 14.65 nm and 13.24 nm respectively.

Morphological properties using FESEM

Figs. 2(a), 2(b) 2(c) and 2(d) show the FESEM images of samples S1, S2, S3 and S4 respectively. The inset in each FESEM represents the image at lower magnification.

Table 2 gives details regarding morphology of nanostructures associated with the samples S1, S2, S3 and S4.

Major portion of the powder sample S1 consists of nanorods (Fig. 2(a)) and remaining portion of the powder consists of elliptical or spherical shaped nanoparticles. Well faceted hexagonal shaped rods with pyramidal shapes (6 faces) at both ends are clearly indicated in Fig. 2(a). This morphology is matching well with wurtzite hexagonal structure of ZnO nanorods. Powder sample S1 was the result of immediate precipitation. Precipitation was

resulted in first 15 minutes. Nanorods found in precipitate may be due to preferential orientation, high mobility of Zn^{2+} and O^{2-} ions and fast growth along c axis. Elliptical shaped nanoparticles may be the indication of the tendency of ZnO to grow preferentially along c axis. Nanorods of good aspect ratio (9.6) were obtained in sample S1.

Elliptical shaped nanoparticles as well as nanorods are the constituents of sample S2 (Fig. 2(b)). The nanostructures were resulted from soft gel. It may be due to better mobility to building blocks (Zn^{2+}, O^{2-} or smaller nuclei) to reach to growth sites of nanorods. Aspect ratio up to 7.0 was possible in this process.

Major portion of powder sample S3 is made up of spherical and elliptical shaped nanoparticles and remaining portion is made up of nanorods and hexagonal platelets as indicated in FESEM image (Fig.2(c)). Maximum value of aspect ratio was found to be 2.31. Lower aspect ratio may be due to smaller mobility of feed material (Zn^{2+}, O^{2-}) in dense gel from which the sample S3 was derived.

Effect of relatively large amount of DMA (20 ml) in zinc acetate (40 ml) was observed in case of sample 4 (ratio of DMA:ZA solution- 1:2). The aging time of gel was too long (21 days). The sol-gel product in beaker was observed to be very soft. Therefore, the mobility of feed material (Zn^{2+}, O^{2-}) would have been larger forming nanorods in powder. Maximum value of the aspect ratio was observed to be largest (12) as compared to other samples.

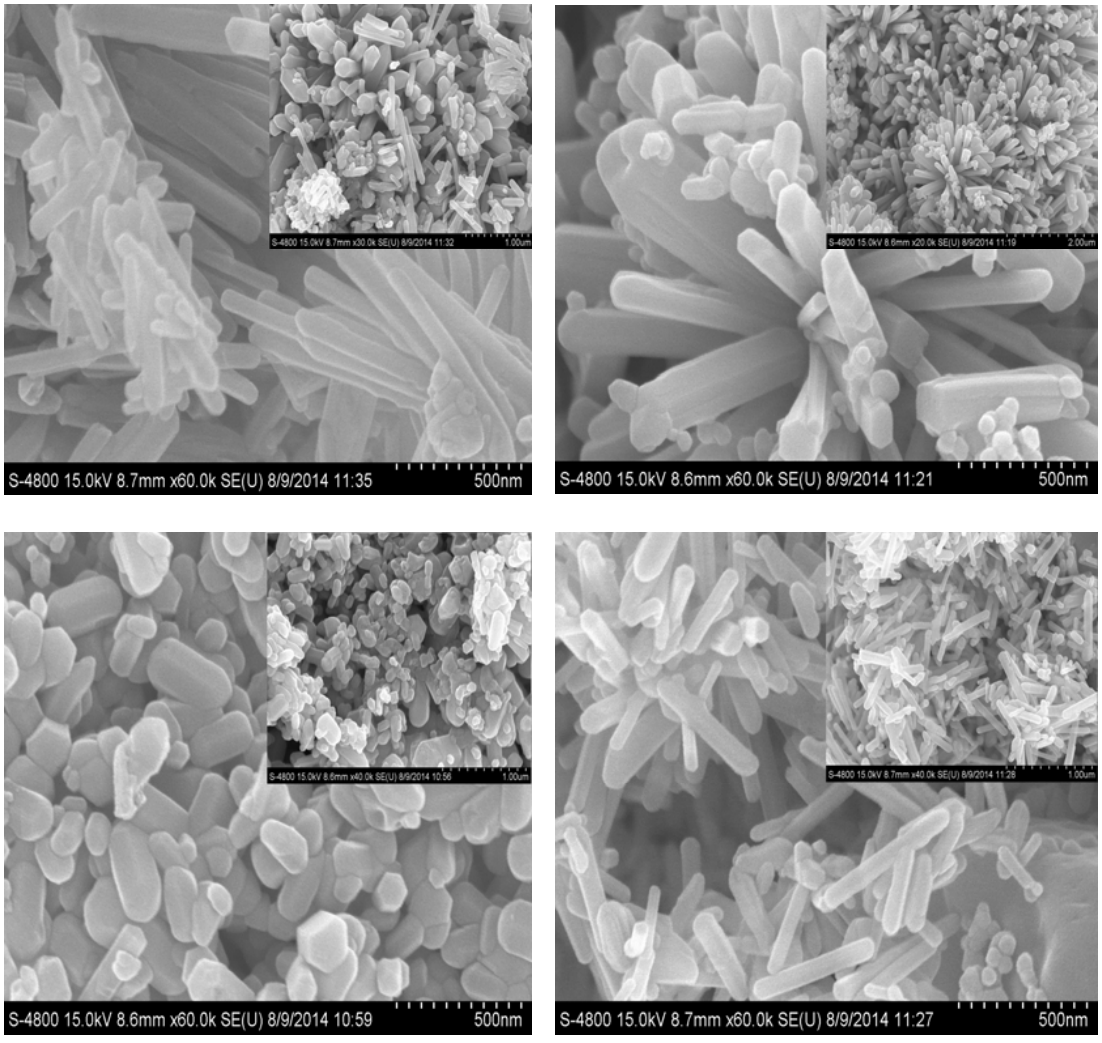

Fig. 2. (a) FESEM image of sample S1 (b) FESEM image of sample S2 (c) FESEM images of sample S3 (d) FESEM images of sample S4

Table 2. gives details regarding morphology of nanostructures associated with the samples S1, S2, S3 and S4.

Sample Name	Morphology of Nanostructures in ZnO powder		Aspect Ratio	
	Major portion of the powder	Minor portion of the powder	Maximum	Minimum
S1	Nanorods	Elliptical/ Spherical nanoparticles	9.6	3.3
S2	Nanorods	Elliptical/ Spherical nanoparticles	7.0	2.0
S3	Elliptical/ Spherical nanoparticles	Nanorods	2.3	1.4
S4	Nanorods	Elliptical/ Spherical nanoparticles	12.0	7.0

Energy Dispersive Analysis by X-rays (EDAX)

The quantitative analysis of samples was made using EDAX arrangement attached to FESEM. Table 3 shows the atomic percentage (at%) of zinc and oxygen constituent ions present in each ZnO sample. Stoichiometrically expected atomic percentage (at%) of zinc and oxygen constituent ions in ZnO is: Zn^{2+} = 50% and O^{2-} = 50%. It is clear from Table 3 that the samples S2 and S4 are stoichiometric and samples S1 and S3 are nonstoichiometric with oxygen deficiency. Almost all peaks associated with EDAX curves are ascribed to Zn and O elements. Thus the as-synthesized samples are composed of Zn and O elements only which is in good agreement with XRD.

The ZnO nanostructured powder samples S2 and S4 were obatined from soft gel which may facilitate higher mobility of growth spaces (Zn^{2+}, O^{2-}) to reach to growth sites of nanostructures associated with them and may establish the stoichiometric levels forming stoichiometric powders. The powder sample S1 was resulted due to fast process of precipitation and there would have been insufficiet time for growth spaces (O^{2-}) to reach to growth sites resulting into non-stoichiometry in terms of oxygen deficiency. The sample S3 was obtained from properly formed high density gel. The mobility of oxygen growth spaces (O^{2-}) to reach to growth sites would have been relatively lower due to high density of gel resulting into non-stoichiometry in terms of oxygen deficiency.

Morphological properties using TEM

Figs. 3(a), 3(b) and 3(c) show the TEM images of sample S1 and Figs. 3(d), 3(e) and 3(f) show the TEM images of sample S3.

It is clear from TEM images that the particles associated with the powder samples S1 (Figs. 3(a) and 3(b)) and S3 (Figs. 3(d), 3(e)) are nanostructures. It can be seen that the powders mainly consists of solid rod like structures. The length of a typical rod in Fig. 3 (b) is around 600 nm and the diameter is around 60 nm. Fig. 3 (d) shows short nanorods or elongated nanoparticles. Figs. 3 (c) and 3(f) are the TEM images indicating electron diffraction from S1 and S3 nanostructure powder samples respectively. Electron diffraction from associated particles is the evidence of crystalline nature of the nanoparticles. HRTEM image in Fig. 3 (e) shows parallel fringes indicating inter planes perpendicular to the [0001] orientation of the nanorods. The inter planer distance (as indicated in Fig. 3(e)) was observed to be 0.37 nm. The measured inter planer distance is observed to be larger than the expected (0.28 nm). It may be due to nonstoichiometry of S3 sample.

Table 3. Quantitative elemental analysis of powder samples.

Sample Name	**at %**		**Stoichiometry**
	Zn^{2+}	**O^{2-}**	
S1	66.98	33.02	Non-stoichiometric (Oxygen deficient)
S2	49.90	50.10	Stoichiometric
S3	58.98	41.02	Non-stoichiometric (Oxygen deficient)
S4	50.63	49.37	Stoichiometric

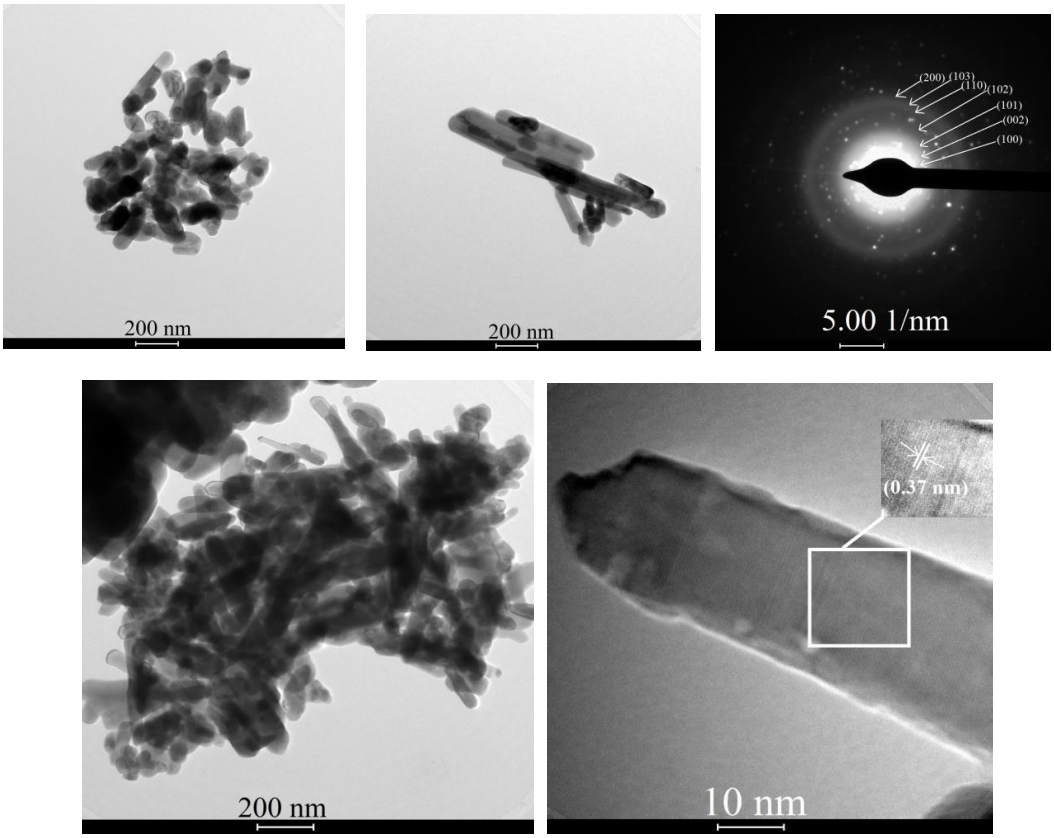

Fig. 3. (a), 3(b), 3(c), 3(e) and 3(f): TEM images of sample S1.

Optical Properties of the ZnO samples

The UV-Vis absorbance spectra of ZnO samples are shown in Fig 4. The band gap energies (Eg) of S1, S2, S3 and S4 samples were observed to be : 3.47 eV, 3.42 eV, 3.4 eV and 3.47 eV respectively. Observed values of band gap energies (Eg) are larger than reported value (Eg= 3.3 eV). The blue shift in absorption edge may be due to nanocrystalline nature of all ZnO samples.

Photoluminiescence (PL) Studies

Fig. 5 represents the room temperature PL spectra of S1, S2, S3 and S4 samples with excitation wavelength of 310 nm. The photoluminiescence peaks between 352 to 360 nm (very weak) may correspond to ultraviolet emmision due to decay of electrons in conduction band to holes in valance band. The peak at 409 nm may be due to near band emmision (NBE). The PL peaks arising in the range 423-460 nm (423nm, 446nm, 460nm) in the samples may be attributed to doubly ionized Zn vacancies (Vzn^{2-}). The peak at 484 nm gives green emmision and it may be due to deep donar states of oxygen vacancies (Vo). The weaker peak at 518 nm may also corresponds to green emmision due to oxygen vacancies (Vo). The peak 542 nm may be due to deep level defects: O_{zn} or O_i. The PL peaks at 564 nm and 571 nm give yellow emmision and may be due to ionized O_i transioin [34].

Growth Mechanism of ZnO nanorods

Synthesis of solid materials via sol-gel process often involves wet chemistry reactions. In sol-gel process, a molecular precursor in homogeneous solution undergoes a succession of transformations: (i) hydrolysis of molecular precursor, (ii) polymeraization via successive addition of ions – forming hydroxyl, (iii) condensation by dehydration, (iv) nucleation and (v) growth. In presnt investigation, DMA was used as an additive in zinc acetate solution for obtaining ZnO nanorods from sol-gel process. DMA reacts with precursor, facilitates the formation of complexes, promotes and stabilizes the sol. The ZnO nanorods were synthesized by precipitation / by sol-gel depending upon the amount od DMA

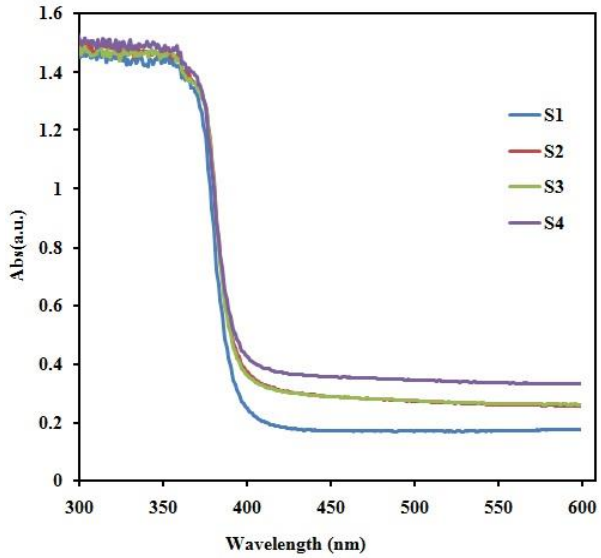

Fig. 4. UV-Vis absorbance spectra of S1, S2, S3 and S4 ZnO samples.

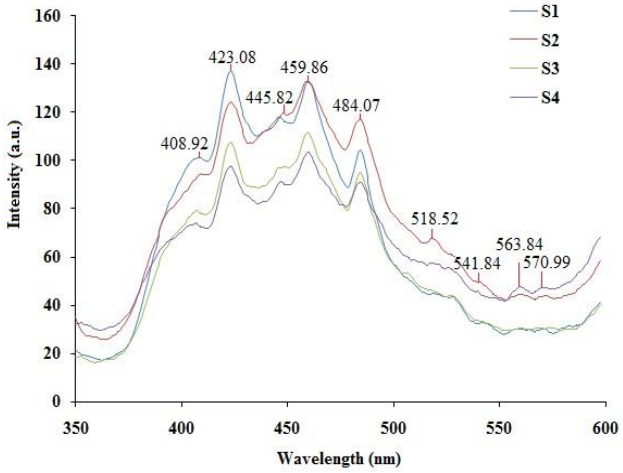

Fig. 5. Photoluminiescence spectra of S1, S2, S3 and S4 ZnO samples.

added into zinc acetate solution. The mechanism of formation of ZnO nanorods and their formation mechanism may be demonstrated by schemes given in equations (2-8) below:

Ionization of precursors: Zinc acetate, DMA and water.

$$(CH_3)_2NH + H_2O \rightarrow (CH_3)_2\,H_2N^+ + OH^- \quad (2)$$

Hydrolysis: Hydrolysis of Zinc acetate becomes more pronounced in presence of DMA

$$Zn(CH_3COO)_2 + OH^- \rightarrow Zn(OH)\,(CH_3COO) + CH_3COO^- \quad (3)$$

$$Zn(OH)\,(CH_3COO) + OH^- \rightarrow Zn(OH)_2 + CH_3COO^- \quad (4)$$

$$Zn(OH)_2 + 2\,OH^- \leftrightarrow [Zn\,(OH)_4]^{2-} \quad (5)$$

Condensation

$$[Zn\,(OH)_4]^{2-} + (CH_3)_2\,H_2N^+ \rightarrow (CH_3)_2\,H_2N^+ - [Zn\,(OH)_4]^{2-} \quad (6)$$

$$(CH_3)_2\,H_2N^+ - [Zn\,(OH)_4]^{2-} \rightarrow ZnO + H_2O + 2OH^-_{(aq)} + (CH_3)_2\,H_2N^+$$

$$[Zn(OH)_4]^{2-}{}_{(aq)} \rightarrow ZnO_{(s)} + 2OH^-_{(aq)} + H_2O_{(aq)} \quad (8)$$

The $[Zn\,(OH)_4]^{2-}$ ions would be produced (rather than $Zn(OH)_2$ precipitates) when amount of DMA solution added into the solution of zinc

acetate (40 ml) was more than 5 ml (6 ml, 8 ml, 20 ml). Notably, the $[Zn(OH)_4]^{2-}$ ions may exist as spherical clusters because of steric effects and the hydrophilicity of the hydroxyl groups. Next, ZnO is formed in addition to two hydroxyl ions and one water molecule. The ZnO nuclei coalesce in order to decrease the total surface energy of the system. These agglomerates grow to form ZnO (Reactions: 5, 6, 7 and 8).

When 5ml DMA solution was added into the solution of zinc acetate (40ml), $Zn(OH)_2$ precipitation would be obtained (Reaction 4).
The condensation of two molecules of $Zn(OH)_2$ may be expressed as (eqs 9-11) :

$$HO\text{-}Zn\text{-}OH + HO\text{-}Zn\text{-}OH \rightarrow HO\text{-}Zn\text{-}O\text{-}Zn\text{-}OH + H_2O \quad (9)$$

For three molecules of $Zn(OH)_2$,

$$HO\text{-}Zn\text{-}O\text{-}Zn\text{-}OH + HO\text{-}Zn\text{-}OH \rightarrow HO\text{-}Zn\text{-}O\text{-}Zn\text{-}O\text{-}Zn\text{-}OH + H_2O$$

For n molecules of $Zn(OH)_2$, there will be poly-condensation as follows:

$$HO\text{-}(Zn\text{-}O\text{-}Zn)_{n-1}\text{-}OH + HO\text{-}Zn\text{-}OH \rightarrow HO\text{-}(Zn\text{-}O\text{-}Zn)_n\text{-}OH + H_2O$$

The samples S1, S2, S3 and S4 were dried at 200 ^{0}C and heated at 500 ^{0}C for 1 h to obtain nanostructured ZnO powder (eq. (12)).

$$\text{Reaction product} \xrightarrow{500\,^\circ C} n\,ZnO + H_2O \quad (12)$$

Reactions 2 and 3 represent an ionization of zinc acetate and DMA molecules. DMA triggers dissociation of water molecules into H^+ and OH^- ions at low temperature (60 ^{0}C). OH^- ions are most important to initiate hydrolysis of zinc acetate to form $[Zn(OH)_4]^{2-}$ ions (Reactions 4 and 5). $[Zn(OH)_4]^{2-}$ exists in the form of negatively charged tetrahedrons, whereas DMA exists in the form of positively charge ions. In neutral or weakly basic solution, the starting material $Zn(OH)_2$ dissolve to smaller extent and dissolve part exists in the form of $[Zn(OH)_4]^{2-}$ (reaction 5). Polarity and basicity of DMA tend to induce formation of tetrahedral shaped $[Zn(OH)_4]^{2-}$. Zinc hydroxide formed in reaction tends to continuously produce Zn^{2+} and O^{2-} ions which form the ZnO nuclei. The nuclei gradually grow in lateral as well as in longitudinal directions. Basal planes ((0001) and (0001)) of hexagonal wurtzite crystals have minimum energy associated with them. This may be the driving force for growing the crystallites along c- axis and result into nanorods. Growth rate of basal planes would be larger as compared to the planes forming hexagonal rods. According to the growth habits of ZnO crystals, it is bounded by positively charged Zn terminated (0001) top facet, negatively charged O terminated (0001) bottom facet and six (0110) side facets. Positively charged and negatively charged polar faces attract newly formed zinc oxide $[Zn(OH)_4]^{2-}$ species as well as OH^- ions towards it. The growth units like polaron, are easy to incorporate on positively charged Zn terminated (0001) and negatively charged O terminated (0001) surfaces due to dipole interaction. So, polar faces grow along c-axis resulting into nanorods. The difference of surface energy of each face of ZnO polar crystal leads to the coalescence of primary particles in specific crystallographic orientation such as one directional growth forming larger secondary particles as evidenced in the formation of ZnO nanorods. Growth of ZnO nanorods may be due to coalescence and oriented attachment (OA) [35] of primary particles.

ZnO nanorods of high aspect ratio were possible using DMA controlled sol-gel process. The variation of DMA as an additive in sol-gel process has changed the length and diameter (aspect ratio) of the nanorods. Depending upon the amount of DMA added into zinc acetate solution, the precipitate, soft gel or properly formed dense gel resulted. Majority of the particles were spherical or elliptical shaped in properly set dense gel and minority were the nanorods. In soft gel or in precipitate, majority of the particles were the nanorods and minority were the spherical or elliptical shaped particles. Thus, by controlling the viscosity of sol-gel with the use of DMA, diffusion and hence mobility of growth units, spherical nanoparticles, elliptical spheroids, or wurtzite structured hexagonal nanorods with [0001] orientation may be synthesized. DMA accelerates the growth units (Zn^{2+} and O^{2-}) and leads to their oriented growth. Growth of ZnO particles with various morphologies may be correlated the fact that when concentration of amine increases, viscosity of liquid phase decreases and thus diffusion rate of growth species increases. When concentration of DMA increases, viscosity of liquid phase would decrease and thus diffusion rate of growth species would increase.

DMA also acts as microsurfactant. Due to its surfactant property, surface tension of solution reduces which decreases the energy needed to form a new phase. Reduction in surface energy is the primary driving force for oriented attachment (OA) based growth. Therefore, nucleation of

ZnO could be possible in lower supersaturation. Initially, ZnO would nucleate in the form of very small elongated nanoparticles. Morphology of the crystallites grown under this condition would be the nanorods as shown in FESEM images.

The texture coefficient of the samples calculated from XRD spectra are observed to be larger than the texture coefficient (0.5) of randomly oriented material. These observations also support the preferential orientation along c axis and hence the growth of ZnO nanorods. Blue shift of absorption edge also gives evidence of nanocrystalline nature of nanorods.

Few of the particles associated in S1, S2 ,S3 and S4 samples (as depicted in FESEM images) are observed to be elliptical or spherical nanoparticles. Elliptical nanoparticles represent the tendency of ZnO to grow along c direction. Size of spherical particles, as clearly seen in FESEM images, is observed to be very small. Such particles would have not got sufficient feed in turns of Zn^{2+} or O^{2-} to grow enough to represent themselves as larger elliptical nanostructures or nanorods.

CONCLUSIONS

In summary, ZnO nanorods of high aspect ratio were synthesized using DMA controlled sol-gel process. DMA is simple amine but found to be very effective to control the aspect ratio of nanorods. The variation of DMA as an additive in sol-gel process changed the length and diameter (aspect ratio) of the nanorods. Depending upon the amount of DMA added into zinc acetate solution, the precipitate, soft gel or properly formed dense gel was resulted. Majority of the nanostructures present in powder were spherical or elliptical shaped nanoparticles in properly set dense gel and minority were the nanorods. In soft gel or in precipitate, majority of the nanostructures were the nanorods and minority were the spherical or elliptical shaped nanoparticles. Thus, by controlling the mobility of growth units (Zn^{2+} and O^{2-}) with the use of DMA, nanoparticles, elliptical spheroids, or wurtzite structured hexagonal nanorods with [0001] orientation may be synthesized. Observed aspect ratio was more than 0.5, indicated the preferential growth along c-axis. The blue shift in absorption edge indicated the nanocrystalline nature of the particles associated in all samples. Use of DMA as an additive in sol-gel process influenced structural, morphological, optical and photoluminescence properties of ZnO nanostructures.

ACKNOWLEDGEMENTS

Authors are thankful to the Head, Department of Physics and also to Principal, Pratap College Amalner for proving research facilities for this investigation. One of the authors (Miss D.G.Patil) is thankful to Department of Science and Technology (DST) for providing the INSPIRE Fellowship.

CONFLICT OF INTEREST

The authors declare that there are no conflicts of interest regarding the publication of this manuscript.

REFERENCES

1. Vajargah PH, H., Ebrahimifard R., Golobostanfard MR, Sol–gel derived ZnO thin films: Effect of amino-additives, Appl. Surf. Sci., 2013; 285P: 732-743.
2. Yan C, Xue D, Conversion of ZnO Nanorod Arrays into ZnO/ZnS Nanocable and ZnS Nanotube Arrays via an in Situ Chemistry Strategy, J.Phy. Chem. B., 2006; 110: 25850-25855.
3. Yan C, Xue D, Electroless deposition of aligned ZnO taper-tubes in a strong acidic medium, Electrochem. Commun. 2007; 9: 1247-1251.
4. Wen B, Huang Y, Boland JJ, Controllable Growth of ZnO Nanostructures by a Simple Solvothermal Process, J. Phy. Chem. C., 2008; 112: 106-111.
5. Yin YT., Que WX, Kam CH, ZnO nanorods on ZnO seed layer derived by sol–gel process, J. Sol-Gel Sci Tech., 2010; 53: 605-612.
6. Law M, Greene LE, Johnson JC, Saykally R, Yang PD, Nanowire dye-sensitized solar cells, Nat. Mater., 2005; 4: 455–459.
7. Liang S, Sheng H, Liu Y, Hiu Z, Lu Y, Shen H, ZnO Schottky ultraviolet photodetectors, J. Cryst. Growth., 2001; 225: 110–113.
8. Saito N, Haneda H, Sekiguchi T, Ohashi N, Sakaguchi I, Koumoto K, Low-Temperature Fabrication of Light-Emitting Zinc Oxide Micropatterns Using Self-Assembled Monolayers, Adv. Mater., 2002; 14: 418–421.
9. Huang MH, Mao S, Feick H, Yan H, Wu Y, Kind H, Weber E, Russo R, Yang P, Room-Temperature Ultraviolet Nanowire Nanolasers, Science, 2001; 292: 1897–1899.
10. Koch MH, Timbrell PY, Lamb RN, The influence of film crystallinity on the coupling efficiency of ZnO optical modulator waveguides, Semicond. Sci. Tech., 1995; 10: 1523–1527.
11. Golego N, Studenikin SA, Cocivera M, Sensor Photoresponse of Thin-Film Oxides of Zinc and Titanium to Oxygen Gas, J. Electrochem. Soc., 2000; 147: 1592–1594.
12. Ge MY, Wu HP, Niu L, Liu JF, Chen SY, Shen PY, Zeng YW, Wang YW, Zhang GQ, Jiang JZ, Nanostructured ZnO: From monodisperse nanoparticles to nanorods, J. Cryst. Growth., 2007; 305: 162-166.
13. Huang MH, Wu Y, Feick H, Tran N, Weber E, Yang P, Catalytic Growth of Zinc Oxide Nanowires by Vapor Transport, Adv. Mater., 2001; 13: 113-116.
14. Vayssieres L, Growth of Arrayed Nanorods and Nanowires of ZnO from Aqueous Solutions, Adv. Mater., 2003; 15: 464-466.
15. Pan ZW , Dai ZR , Ma Chris, Wang ZL, Molten Gallium as a

Catalyst for the Large-Scale Growth of Highly Aligned Silica Nanowires, J. Am. Chem. Soc., 2002; 124: 1817-1822.
16. Ng HT, Li J, Smith MK, Nguyen P, Cassell A, Han J, Meyyappan M, Growth of epitaxial nanowires at the junctions of nanowalls, Science, 2003; 300: 1249.
17. Umar A, Kim SH, Lee YS, Nahm KS, Hahn YB, Catalyst-free large-quantity synthesis of ZnO nanorods by a vapor–solid growth mechanism: Structural and optical properties, J. Cryst. Growth., 2005; 282: 131-136.
18. Kong YC, Yu DP, Zhang B, Fang W, Feng SQ, "Ultraviolet-Emitting ZnO Nanowires Synthesized by a Physical Vapor Deposition Approach," Appl. Phy. Lett., 2001; 78: 407- 409.
19. Lyu SC, Zhang Y, Ruh H, Lee HJ, Shim HW, Suh EK, Lee CJ, Low temperature growth and photoluminescence of well-aligned zinc oxide nanowires, J. Chem. Phys. Lett., 2002; 363: 134-138.
20. Lee DJ, Park JY, Yun YS, Hong YS, Moon JH, Lee BT, Kim SS, Comparative studies on the growth behavior of ZnO nanorods by metalorganic chemical vapor deposition depending on the type of substrates, J. Cryst. Growth., 2005; 276: 458-464.
21. Park WI, Kim DH, Jung SW, Yi GC, Metalorganic vapor-phase epitaxial growth of vertically well-aligned ZnO nanorods, Appl. Phys. Lett., 2002; 80: 4232-4234.
22. Park JY, Lee DJ, Kim SS, Size control of ZnO nanorod arrays grown by metalorganic chemical vapour deposition, Nanotech., 2005; 16: 2044-2047.
23. Li Y, Meng GW, Zhang LD, Phillip F, Ordered Semiconductor ZnO Nanowires Arrays and Their Photoluminescence Properties, Appl. Phys. Lett., 2000; 76: 2011-2013.
24. Cheng JP, Zhang XB, Tao XY, Lu HM, Luo ZQ, Liu F, Fine-Tuning the Synthesis of ZnO Nanostructures by an Alcohol Thermal Process, J. Phys. Chem. B, 2006; 110: 10348-10353.
25. Peng W, Qu S, Cong G, Wang Z, Synthesis and Structures of Morphology-Controlled ZnO Nano- and Microcrystals, Cryst. Growth. Design., 2006; 6: 1518-1522.
26. Cao HL, Qian XF, Gong Q, Du WM, Ma XD, Zhu ZK, Shape- and size-controlled synthesis of nanometre ZnO from a simple solution route at room temperature, Nanotech., 2006; 17: 3632-3636.
27. Liu RL, Xiang Q, Pan QY, Cheng ZX, Shi LY, Hydrothermal synthesis and gas sensitivity of one-dimensional zinc oxide. Chin.J. Inorg. Mater., 2006; 21: 793-796.
28. Tam KH, Cheung CK, Leung YH, Djurišić AB, Ling CC, Beling CD, Fung S., Kwok WM, Chan WK, Phillips DL, Ding L, Ge WK, Defects in ZnO Nanorods Prepared by a Hydrothermal Method, J. Phys. Chem. B., 2006; 110: 20865-20871.
29. Voggu R, Biswas K, Govindaraj A., Rao C. N. R., Use of Fluorous Chemistry in the Solubilization and Phase Transfer of Nanocrystals, Nanorods, and Nanotubes, J. Phys. Chem. B., 2006; 110: 20752-20755.
30. Tong Y, Liu Y, Dong L, Zhao D, Zhang J, Lu Y, Shen D, Fan X, Growth of ZnO Nanostructures with Different Morphologies by Using Hydrothermal Technique, J. Phys. Chem. B., 2006; 110: 20263-20267.
31. Chen Y, Kim M, Lian G, Johnson MB, Peng X, Side Reactions in Controlling the Quality, Yield, and Stability of High Quality Colloidal Nanocrystals, J. Am. Chem. Soc., 2005; 127: 13331-13337.
32. Spanhel L, Anderson MA, Semiconductor clusters in the sol-gel process: quantized aggregation, gelation, and crystal growth in concentrated zinc oxide colloids, J.Am.Chem. Soc., 1991; 113: 2826-2833.
33. Kajikawa Y, Noda S, Komiyama H, Preferred Orientation of Chemical Vapor Deposited Polycrystalline Silicon Carbide Films, Chem. Vapour Deposition, 2002; 8: 99.
34. Biroju RK, Giri PK, Dhara S, Imakita K, Fujii M, Graphene-Assisted Controlled Growth of Highly Aligned ZnO Nanorods and Nanoribbons: Growth Mechanism and Photoluminescence Properties, Appl. Mater. Interfaces, 2014; 6: 377-387.
35. Zhang Q, Liu SJ, Yu SH, Recent advances in oriented attachment growth and synthesis of functional materials: concept, evidence, mechanism, and future, J. Mater. Chem., 2009; 19: 191.